DOI 10.24425/aee.2023.143696

# Generalized state space model and small signal stability analysis of Z-source converter

MASOUD JOKAR KOUHANJANI[1] ✉, SINA SOLTANI[2], MOHAMMAD MARDANEH[3]

[1]*Department of Technical Study*
*Shiraz Electric Distribution Company*
*Shiraz, Iran*

[2]*Department of Control and Management*
*Neyriz Ghadir Steel Complex (NGHSCO)*
*Fars, Iran*

[3]*Department of Power and Control Engineering*
*Shiraz University of Technology*
*Shiraz, Iran*

*e-mail:* ✉*masoudjokar@hotmail.com, sinasoltani@shirazu.ac.ir, mardaneh@sutech.ac.ir, mail4*

(Received: 23.08.2022, revised: 04.11.2022)

**Abstract:** This paper proposes two nonlinear exact and simple state space models of a Z-source converter (ZSC) connected to an ac grid. A generic model of a ZSC accompanied with proper controllers are proposed and a dynamic model of the whole system is derived; as a result, based on a simple one, an equivalent block diagram of the current-controlled ZSC system is proposed. The ac small signal stability method is applied and the impact of controller parameters on network's stability is discussed. Besides, overall system dynamic performance has been assessed in the event of perturbations. Time-domain simulations have been implemented in PSCAD/EMTDC to validate the accuracy of the models and effectiveness of the proposed controllers. The results of the exact model are compared with the response of the equations which are applied in MATLAB.

**Key words:** small signal stability, state space model, Z-source converter (ZSC)

## 1. Introduction

A Z-source converter, a novel replaceable energy conversion topology that is equipped by passive components, has been proposed in [1]. Various topologies, control and modulation strategies are considered in [2, 3], respectively. In contrast with conventional voltage-source converters

(VSCs) and current-source converters (CSCs), the specific characteristic of ZSCs is both buck and boost capabilities which is the outcome of:

i) shoot through switching state, at least two switches of one leg are on,

ii) X-shaped impedance network that includes two inductors ($L_1$ and $L_2$) and two capacitors ($C_1$ and $C_2$), as well as the connection between a dc power source and a set of switches, as shown in Fig. 1.

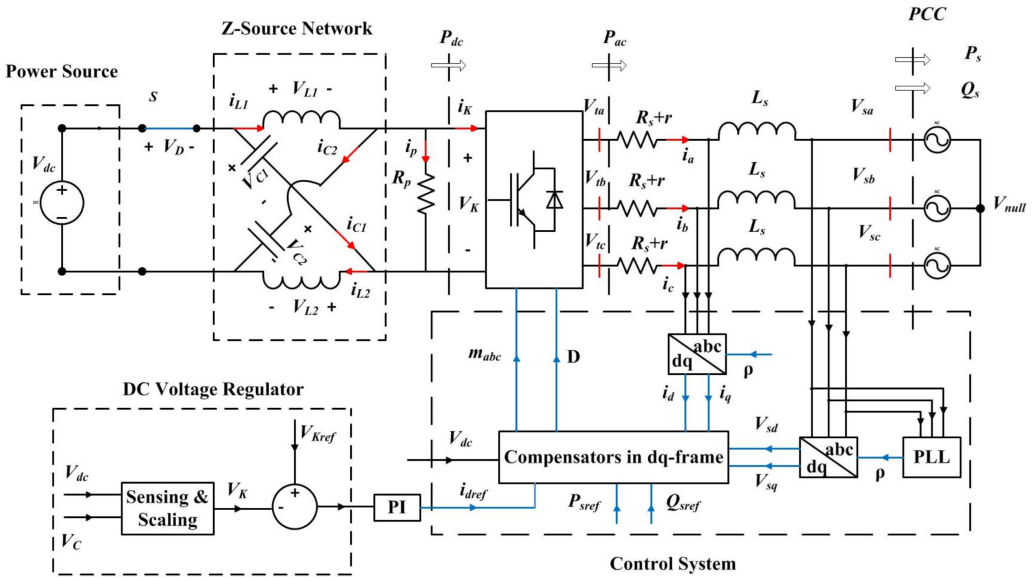


Fig. 1. Generic model of ZSC connected to ac grid

Nowadays, there is an extension to the power system to utilize power electronic-based equipment such as: distributed generation (DG) units, HVDC lines and FACTS. Furthermore, due to the remarkable capability of ZSCs that allows them to work as a buck or boost converter relevant to desired DC-bus or ac terminal voltages, there will be a wide usage of ZSCs instead of VSCs in the near future, particularly in the case of a power source with conversional output terminal voltage. A large number of literatures have been allocated to various uses of ZSCs, which is clear evidence of the steep increase in research on finding various suitable applications for this novel converter, e.g., for adjustable-speed drives [4,5], electric vehicles [6–9], distributed generation [10–15] and so on. In order to perform a feasibility study and detailed design, a precise comprehensive model of the entire considered system should be provided.

Publications related to the model of Z-source converters mostly concentrate on the circuit of the converters with a simple load regardless of the dynamic behavior of the ac grid and without considering active and reactive power controllers [16–19]. In [20], a steady state analysis of a Z-source dc-ac converter operating in continuous conduction mode (CCM) is presented. The circuit-averaging technique is used to present ac small-signal modeling of the power stage of a Z-source converter in [21].

In this paper, a Z-source dc-ac converter equipped with proper active and reactive power controllers and connected to the infinitely stiff ac grid, which has constant frequency and balanced sinusoidal voltage, is considered. The rest of this paper is organized as follows. In Section 2, state space equations of electrical circuits, an impedance network and the ac grid, are derived. Moreover, a coupling equation that makes relation between the impedance network and the ac grid is derived. In order to track the desired active and reactive power a suitable control system is proposed in Section 3, according to the conventional control methodology that is widely used in VSCs. Section 4 is allocated to show the simplified model. Subsequently, the ac small-signal stability method is applied in Section 5 in order to analyze the stability of the system and propose an equivalent block diagram of the system. Section 6 is allocated to show the time-domain simulation which is implemented in Matlab. The results are compared to the exact switching circuit developed in PSCAD/EMTDC. Finally, Section 7 concludes the paper and comments on possible future works.

## 2. Dynamic equations of electrical circuit

Figure 1 represents the included ZSC impedance network with a set of IGBTs, and its corresponding ac-side equivalent circuit. There are four well-known methods to implement the PWM switching strategy for Z-source converters: simple constant boost applied in this study [1], maximum boost [22], maximum constant boost [23] and the triangle-shift control strategy [24]. The performance region of the converter is shown in Fig. 2. The basic equations of Z-source converter terminal voltage are as follows [1], according to the stated switching function:

$$B_{\max} = \frac{1}{1 - 2D_{\max}}, \tag{1}$$

$$G = M \cdot B = \frac{1 - D}{1 - 2D}, \tag{2}$$

where: $M$ is the buck modulation index, $D$ is the shoot-through duty ratio, $B$ and $G$ are the boost factor and the voltage gain of the converter in inversion mode, respectively. The system comprises a power source that could be the representative of a DG unit, dc link or a part of a back-to-back converter. The resistance $R_p$ represents the total switching loss of the system [25]. The ac side of the converter is connected to a utility grid through a series $RL$ filter and three-phase transformer that are modeled by $R_s$ and $L_s$.The synchronization signals for the control system are taken from the low-voltage side of the corresponding transformer. The ZSC of Fig. 1 exchanges real and reactive power components, $P_s(t)$ and $Q_s(t)$, with the ac grid at the point of common coupling (PCC). For simplicity and without loss of accuracy, we assume the following:

- $V_{\text{dc}}$ is an ideal and independent voltage source. The forward voltage drop of $S_1$ is considered as a constant voltage drop $V_D$. More explanation is delivered in the control system section.
- The carrier frequency is assumed much larger than that of the modulating signal (e.g. more than 10 times).
- The dc capacitors and inductances are adequately large so that the changes of their voltages and currents within one carrier period can be neglected. The impedance network is considered lossless.

– IGBT is presumed fast, therefore, we do not consider a time constant in a switch dynamic model; moreover, in its conducting state, it is modeled by the series resistant ($r$).
– A large number of dynamic models proposed for VSCs in literatures do not take into account an ac-side capacitor filter [25–27].

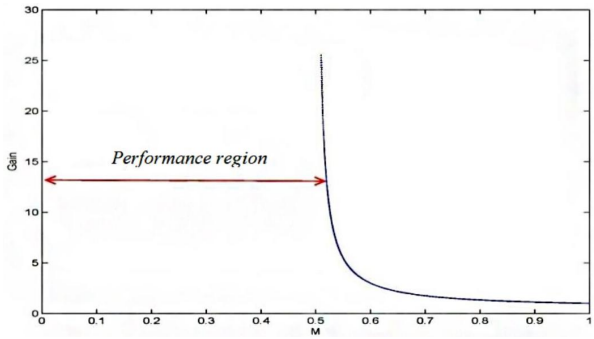


Fig. 2. Capable performance region of ZSC according to simple constant boost switching strategy method

Two operation modes including two different circuit topologies can be introduced in ZSC operation relevant to non-shoot through and shout through states [1, 16] as shown in Fig. 1 and Fig. 3, respectively. Dynamics of the ac side of the ZSC system are described by the following space-phasor equation:

$$L_s \frac{\mathrm{d}\vec{i}}{\mathrm{d}t} = -(R_s + r)\vec{i} + \vec{V}_t - \vec{V}_s\,, \tag{3}$$

where $V_s$ and $V_t$ are the voltages of the power system and ac terminals of the converter, respectively. For the traditional V-source PWM converter, we have the well-known relationship:

$$v_t(t) = M\frac{V_k}{2}\cos(\omega t + \delta). \tag{4}$$

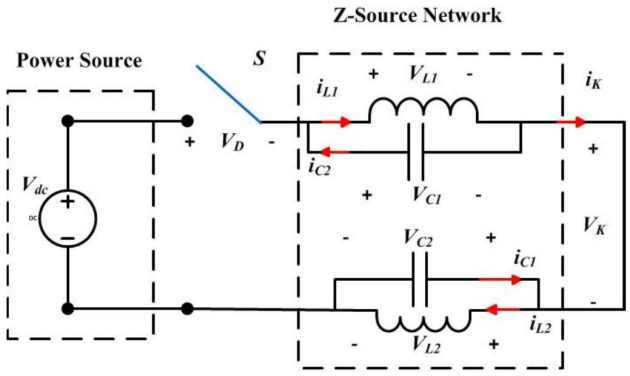


Fig. 3. Equivalent circuit of Z-source converter in the shoot-through state

$V_k$ is the voltage of the dc side terminal of the converter, $M$ is the buck modulation index which is considered constant during operation modes of the ZSC, and $\delta$ is the phase difference

with respect to the grid voltage. For ZSCs we have a relationship between the discontinuous input voltage of the set of switches, ($V_K$), and the voltage of the power source, ($V_{\mathrm{dc}}$):

$$V_k = \frac{1}{1-2D} V_{\mathrm{dc}}\,, \tag{5}$$

where: $V_{\mathrm{dc}}$ stands for the dc source voltage, $D$ and $\dfrac{1}{1-2D}$ are the shoot through and boost factors, respectively. In order to simplify modeling and analysis, all state equations in the *abc* domain are transformed into a *d-q* rotating reference frame. The transformation matrix is given by (4) where "$f$" can be any electrical parameter.

$$\begin{bmatrix} f_d \\ f_q \\ f_0 \end{bmatrix} = \frac{2}{3} \begin{bmatrix} \cos(\omega t) & \cos\left(\omega t - \dfrac{2\pi}{3}\right) & \cos\left(\omega t + \dfrac{2\pi}{3}\right) \\ \sin(\omega t) & \sin\left(\omega t - \dfrac{2\pi}{3}\right) & \sin\left(\omega t + \dfrac{2\pi}{3}\right) \\ \dfrac{1}{2} & \dfrac{1}{2} & \dfrac{1}{2} \end{bmatrix} \begin{bmatrix} f_a \\ f_b \\ f_c \end{bmatrix}. \tag{6}$$

It is assumed that the system is balanced and zero-sequence components do not exist. The angle $\omega t$ is provided by the phase-locked loop (PLL), arbitrarily assumed here to align the system voltage with the *d*-axis. By using *abc* to the *d-q* transformation matrix for the terminal voltage of the converter:

$$V_{tq} = M \frac{V_k}{2} \sin(\delta), \tag{7}$$

$$V_{td} = M \frac{V_k}{2} \cos(\delta). \tag{8}$$

The current of inductances, the voltage of capacitors and the *d-q* components of the grid current are defined as state variables.

$$x(t) = \begin{bmatrix} i_{L1}(t) & i_{L2}(t) & V_{C1}(t) & V_{C2}(t) & i_d(t) & i_q(t) \end{bmatrix}^T. \tag{9}$$

The model of the converter and the ac grid are derived based on two modes of the ZSC operation.

### 2.1. Shoot-through state

In mode 1, no energy is transferred from the source to the load, since the load and the source sides are entirely separated by the shoot-through state (at least one leg of IGBTs are on) and open status of the switch $S$. The duty ratio of the shoot-through state is defined as $d$. Differential equations of the ac grid and impedance network are:

$$L_s \frac{\mathrm{d}i_d(t)}{\mathrm{d}t} = L_s \omega i_q(t) - (R_s + r)\, i_d(t) - V_{sd}(t), \tag{10}$$

$$L_s \frac{\mathrm{d}i_q(t)}{\mathrm{d}t} = -L_s \omega i_d(t) - (R_s + r)\, i_q(t), \tag{11}$$

$$L_1 \frac{\mathrm{d}i_{L1}(t)}{\mathrm{d}t} = V_{C1}(t), \qquad L_2 \frac{\mathrm{d}i_{L2}(t)}{\mathrm{d}t} = V_{C2}(t), \tag{12}$$

$$C_1 \frac{\mathrm{d}V_{C1}(t)}{\mathrm{d}t} = -i_{L1}(t), \qquad C_2 \frac{\mathrm{d}V_{C2}(t)}{\mathrm{d}t} = -i_{L2}(t). \tag{13}$$

As shown in Fig. 3, the switch $S$ is opened and the dc current transferred to the impedance network is zero; therefore, $i_k(t)$, the current that flows through IGBTs, should be zero, which is an advantage for ZSCs.

### 2.2. Non-shoot-through state

In mode 2, real energy is transferred between the source and load. As $i_p$ is assumed constant, we do not consider it in a dynamic model of the converter. The duty ratio of the shoot-through state is defined as $d'$. Similarly, the state equations of the ac grid and impedance network can be written in mode 2 as follows, respectively:

$$\frac{L_s \mathrm{d}i_d(t)}{\mathrm{d}t} = L_s \omega i_q(t) - (R_s + r)\, i_d(t) - V_{sd} + V_{td}(t), \tag{14}$$

$$\frac{L_s \mathrm{d}i_q(t)}{\mathrm{d}t} = -L_s \omega i_d(t) - (R_s + r)\, i_q(t) + V_{tq}(t), \tag{15}$$

$$\frac{L_1 \mathrm{d}i_{L1}(t)}{\mathrm{d}t} = V_{dc}(t) - V_{C2}(t), \qquad \frac{L_2 \mathrm{d}i_{L2}(t)}{\mathrm{d}t} = V_{\mathrm{dc}}(t) - V_{C1}(t), \tag{16}$$

$$\frac{C_1 \mathrm{d}V_{C1}(t)}{\mathrm{d}t} = i_{L2}(t) - i_k(t), \qquad \frac{C_2 dV_{C2}}{dt} = i_{L1}(t) - i_k(t). \tag{17}$$

Finally, the ac and dc circuit equations have to be coupled. The coupling equation follows from the active power balance between the ac and dc sides of the converter. It allows calculating the dc current of the converter:

$$V_k(t) i_k(t) = \frac{3}{2} \left( V_{td}(t) i_d(t) + V_{tq}(t) i_q(t) \right). \tag{18}$$

From KVL in impedance network:

$$V_k(t) i_k(t) = \frac{3}{2} \left( V_{td}(t) i_d(t) + V_{tq}(t) i_q(t) \right). \tag{19}$$

## 3. Control system

The purpose of designing the controller is to achieve good output-active and reactive power tracking which are exchanged with the ac network at PCC. Among various control methods found in the literature: internal model control in [28]; $H_\infty$ controllers in [28, 29]; a control strategy based on the Lyapunov function in [30]; optimal coordinated control of the VSC and ac line in parallel [31], two decouple-loop controllers are proposed for the Z-source inverter [32] through the decoupled current-control method applied in this study, [25–27]. However, the control system is modified so as to accommodate it in the ZSC system, Fig. 4 without $d'$ in the current controller part.

In the case of disregarding variations of the dc source, two individual cases could have occurred.

i) DC source represents an energy source that can meet the active power demand at various ranges of dc voltages by changing the dc current and persisting output dc energy. More profoundly, it can be concluded from Fig. 4 that any changes in $V_{\mathrm{dc}}(t)$ adversely contribute to changes in $D$, leading to no effect in the tracking process of $I_{d\mathrm{ref}}$ and $I_{q\mathrm{ref}}$ values.
ii) The power source is a capacitor which is a part of the dc line or back-to-back converter. Consequently, any changes in dc voltage follow from energy equation disturbance held between input power from the source of energy behind the proposed system, mentioned capacitor and output energy to the Z-source impedance network.

Therefore, the presence of a dc voltage regulator in this case is unavoidable [13]. However, the function of the dc controller is to change the set point of active power demand, as illustrated in Fig 1. In the case of dynamic equations, it causes an extra state which is ignored in this study for simplicity.The real and reactive powers delivered to the ac system at PCC are:

$$P_s(t) = \frac{3}{2} V_{sd} i_d(t), \tag{20}$$

$$Q_s(t) = -\frac{3}{2} V_{sd} i_q(t). \tag{21}$$

From (20) and (21) the reference value of $dq$-components of the current ($I_{d\mathrm{ref}} I_{q\mathrm{ref}}$) can be calculated based on the desired value of active and reactive powers. Therefore, a proportional-integral (PI) compensator of the generic form $K(s) = \left(k_p s + \frac{k_i}{s}\right)$ is sufficient for the control. Due to the presence of $L\omega$ in (14) and (15), dynamics of $i_d(t)$ and $i_q(t)$ are coupled. To decouple (14) and (15), $m_d(t)$ and $m_q(t)$ are determined as follows:

$$m_d(t) = \frac{2\left(u_d(t) + V_{sd} - L_s \omega i_q(t)\right)}{V_{\mathrm{dc}}(t)}, \tag{22}$$

$$m_q(t) = \frac{2\left(u_q(t) + V_{sq} + L_s \omega i_d(t)\right)}{V_{\mathrm{dc}}(t)}, \tag{23}$$

where $u_d(t)$ and $u_q(t)$ are:

$$u_d(t) = \left(k_p + \frac{k_i}{s}\right)\left(i_{d\mathrm{ref}} - i_d(t)\right), \tag{24}$$

$$u_q(t) = \left(k_p + \frac{k_i}{s}\right)\left(i_{q\mathrm{ref}} - i_q(t)\right). \tag{25}$$

We introduce two additional state variables, $z_d(t)$ and $z_q(t)$, such that:

$$\frac{\mathrm{d}z_d(t)}{\mathrm{d}t} = i_{d\mathrm{ref}} - i_d(t), \tag{26}$$

$$\frac{\mathrm{d}z_q(t)}{\mathrm{d}t} = i_{q\mathrm{ref}} - i_q(t). \tag{27}$$

The outputs of the current controllers are $dq$-components of the modulation index, $m_d$ and $m_q$, that include buck and boost factors simultaneously. By transforming the modulation index

from *dq* to the *abc*-frame, two relations are derived according to the following trigonometric relationships:

$$\delta = \tan^{-1}\frac{m_q(t)}{m_d(t)} = \tan^{-1}\frac{u_q(t) + L_s\omega i_d(t)}{u_d(t) + V_{sd}(t) - L_s\omega i_q(t)}, \tag{28}$$

$$\frac{M}{1-2d(t)} = \sqrt{m_d^2(t) + m_q^2(t)}\,. \tag{29}$$

It can be concluded from (28) that the amplitude of the modulation signal, $m_{abc}$ (blue arrows), is more than unity which causes over-modulation; moreover, the control system should calculate a shoot-through coefficient appropriate to the desired value of instantaneous active and reactive power that the ZSC system exchanged with the ac system. Therefore, the shoot-through calculation part is proposed as illustrated in Fig. 4. The buck modulation index ($M$) is arbitrarily chosen to be less than unity. Finally, the *abc*-frame of the modulation signal obtained with an amplitude is equal to $M$.

The impedance network is considered symmetric, that is $L_1 = L_2 = L$ and $C_1 = C_2 = C$. All differential equations can be written in the form of a nonlinear state space equation,

$$\dot{\overline{x}}(t) = \overline{A}\overline{x}(t) + \overline{B}\overline{u}(t) + \overline{N}(x,u),$$

that is:

$$\frac{\mathrm{d}}{\mathrm{d}t}\begin{bmatrix} i_L(t)\\ V_C(t)\\ i_d(t)\\ i_q(t)\\ z_d(t)\\ z_q(t)\end{bmatrix} = \begin{bmatrix} 0 & \frac{d-d'}{L} & 0 & 0 & 0 & 0\\ \frac{d'-d}{C} & 0 & 0 & 0 & 0 & 0\\ 0 & 0 & -\frac{R+r}{L} & -\omega & 0 & 0\\ 0 & 0 & -\omega & -\frac{R+r}{L} & 0 & 0\\ 0 & 0 & -1 & 0 & 0 & 0\\ 0 & 0 & 0 & -1 & 0 & 0\end{bmatrix}$$

$$\begin{bmatrix} i_L(t)\\ V_C(t)\\ i_d(t)\\ i_q(t)\\ z_d(t)\\ z_q(t)\end{bmatrix} + \begin{bmatrix} \frac{d'}{L} & 0\\ 0 & 0\\ 0 & -\frac{1}{L_s}\\ 0 & 0\\ 0 & 0\\ 0 & 0\end{bmatrix}\begin{bmatrix} V_{\mathrm{dc}}(t) - V_D\\ V_{sd}(t)\end{bmatrix} + \begin{bmatrix} 0\\ -\frac{3}{4C}d'M(i_d(t)\cos\left(\delta\,(t) + i_q(t)\sin\left(\delta(t)\right)\right)\\ \frac{d'M}{2L_s}\cos\left(\delta(t)\right)\left(2V_C\,(t) - V_{\mathrm{dc}}(t)\right)\\ \frac{d'M}{2L_s}\sin\left(\delta(t)\right)\left(2V_C\,(t) - V_{\mathrm{dc}}(t)\right)\\ 0\\ 0\end{bmatrix}. \tag{30}$$

where $\overline{N}(x,u)$ is the nonlinear part depending on both state variables and input.

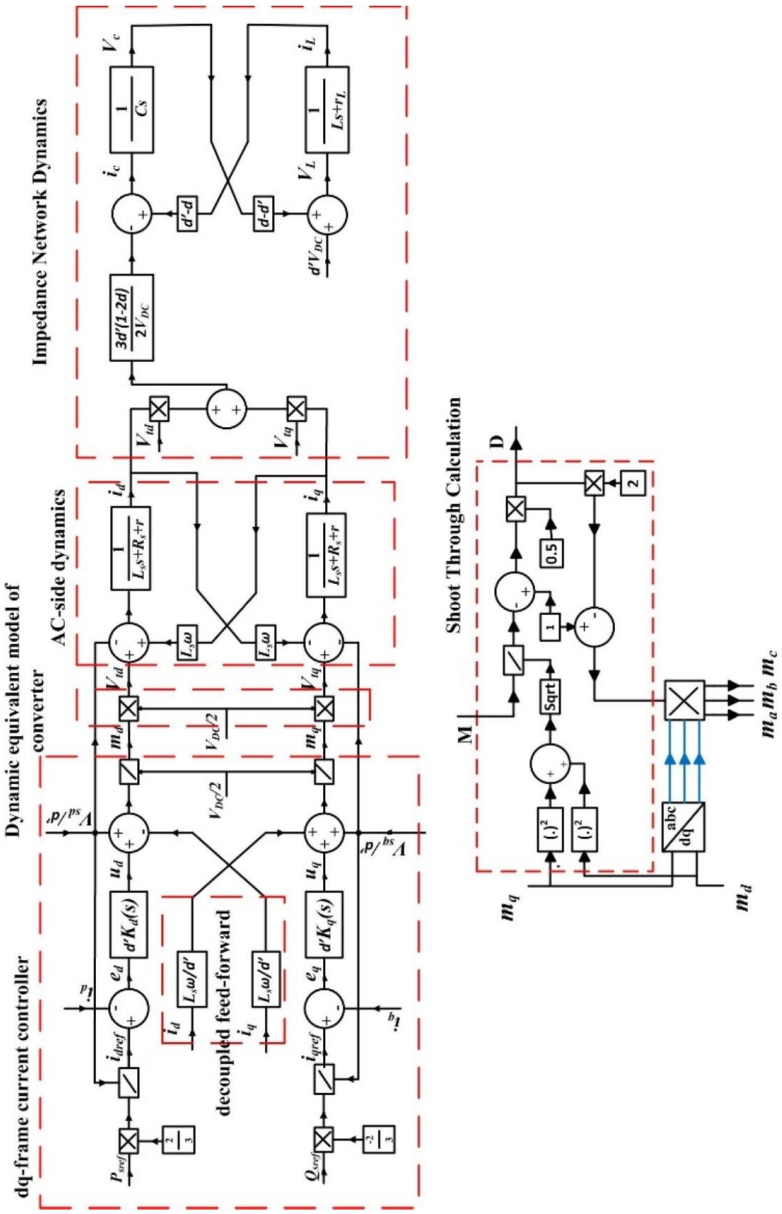


Fig. 4. Control block diagram of current-controlled ZSC system

## 4. Simplified model

So far, a comprehensive dynamic model and ac-side current-controller are proposed. The proposed model is totally nonlinear and undeniably hard to work for stability consideration and to drive related transfer functions for the controller design. Also, it is impossible to opt the value of decoupling feed-forward links in the control system to separate the dynamic behavior of $i_d(t)$ and $i_q(t)$ theoretically complete. Analytically and according to (30), the dynamic behavior of the ac and dc sections is coupled. The chief component responsible for this fact is the impedance network inductance $L$ which provides the main path of the current to the ac-section. More elaborately, in the process of varying the active power setpoint, the dc current has to adapt to the desired value, while the inductance ($L$) is inherently reluctant to rapid changes, contributing to capacitor participation in providing demanded energy at the first moment of changes. On the other hand, the converter deals with reactive power variations more smoothly, since there is no need to change the amount of produced dc energy by means of dc current. The desired amount of reactive power relating tightly to the amplitude of ac terminal voltage of the converter is provided by changes in the capacitor voltage with respect to (19). In addition, as $\delta$ is mostly small, the dynamic response of $i_q(t)$ is less dependent on the impedance network than $i_d(t)$. Regarding this explanation, the dependence of ac-part states on dc network components has been ignored for the sake of simplicity; nevertheless, the dc-section dynamic equations are still inevitably coupled to ac-side parameters. This dependence results from how to define $V_{td}(t)$ and $V_{tq}(t)$. Unlike the previous form defined based on combination of electrical circuit and control system relations in a simplified form, just control system equations, which mostly affect, are considered. Therefore, we have:

$$V_{td}(t) = m_d(t)\frac{V_{\mathrm{dc}}}{2}\,, \tag{31}$$

$$V_{tq}(t) = m_q(t)\frac{V_{\mathrm{dc}}}{2}\,. \tag{32}$$

That is leading to:

$$L_s\frac{\mathrm{d}i_d(t)}{\mathrm{d}t} = -\left(R_s + d'K_p\right)i_d(t) + d'K_i z_d(t) + d'I_{d\mathrm{ref}}K_p\,, \tag{33}$$

$$L_s\frac{\mathrm{d}i_q(t)}{\mathrm{d}t} = -\left(R_s + d'K_p\right)i_q(t) + d'K_i z_q(t) + d'I_{q\mathrm{ref}}K_p\,, \tag{34}$$

$$L\frac{\mathrm{d}i_L(t)}{\mathrm{d}t} = (d-d')\,v_C(t) + d'V_{\mathrm{dc}}(t) - R_L i_L(t), \tag{35}$$

$$\begin{aligned} C\frac{\mathrm{d}v_C(t)}{\mathrm{d}t} = {} & (d'-d)i_L(t) - \frac{3d'(1-2d)}{2V_{\mathrm{dc}}(t)}\Big[i_d(t)K_p(I_{d\mathrm{ref}} - i_d(t)) + i_d(t)z_d(t)K_i \\ & + \frac{V_{sd}i_d(t)}{d'} + i_q(t)z_q(t)K_i + i_q(t)K_q(I_{q\mathrm{ref}} - i_q(t))\Big], \end{aligned} \tag{36}$$

$$\frac{\mathrm{d}z_d(t)}{\mathrm{d}t} = I_{d\mathrm{ref}} - i_d(t), \tag{37}$$

$$\frac{\mathrm{d}z_q(t)}{\mathrm{d}t} = I_{q\mathrm{ref}} - i_q(t). \tag{38}$$

It should be noted that (33), (34) are completely decoupled. In other words, in the simplified model, there is a capability to choose a proper value for decoupling feed-forward links, shown in the controller part of Fig. 4. Moreover, a series resistance is considered in the dynamic equation of the inductance current, due to avoiding instability of dc-side states. In Fig. 4, an impedance network dynamic part is obtained from (35), (36).

## 5. Small signal stability

The small-signal stability of the test system is assessed using eigenvalue analysis in order to find out the nature and root reason for the dynamic response of the ZSC. The simplified model by differential Eqs. (33)–(38) is linearized around a set point of Table 1.

For analyzing the impact of different parameters, root-loci of eigenvalues are sketched according to changes in the value of impedance network elements and current controller parameters independently. As shown in Fig. 5, a pair of poles is under influence of the capacitance and inductance of the dc-side network, while $K_p$ and $K_i$ affect only the other two pair of poles. It can be concluded that:

– High value of impedance network elements leads to decreasing oscillation of dynamic response of all states, but mostly dc-side ones.
– It is potentially achievable to find an appropriate value of current controller parameters, contributing to the order reduction of the system to the dominant poles.

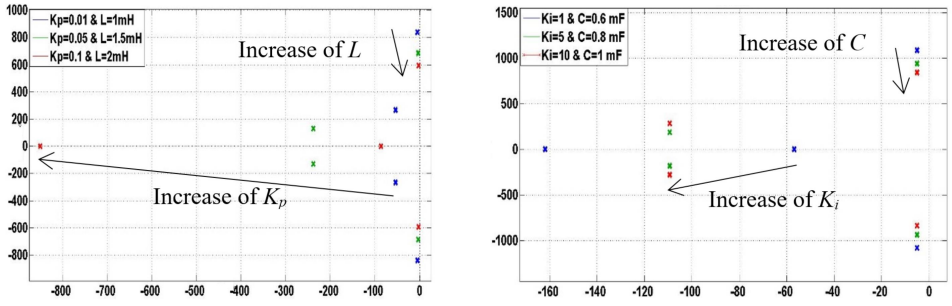


(a) (b)

Fig. 5. Effect of parameters on poles of the system: different inductances and $K_p$ (a); different capacitances and $K_i$ (b)

## 6. Time domain validation

The studies reported in this section were performed on the Z-source converter of Fig. 1 using parameters of Table 1. The studies are conducted:

– To verify the accuracy of the averaged models.
– To demonstrate the performance of the active and reactive power compensator proposed in Section 3.

Three study models of the system of Fig. 1 are simulated. The first one is the switching circuit of the system including the $d$-$q$ frame current controller and shoot-through calculation parts of Fig. 4. This model is implemented in the PSCAD/EMTDC environment. The second and third models are exact and simplified models derived in Sections 2 and 4, respectively. They can be developed in an equation solver environment, e.g. MATLAB.

### 6.1. Models walidation

Initially the converter is delivering 0.1 MW active power to a local load, then at $t = 0.6$ s the breaker of the ac grid is closed and the reference signal of active power changed to 3.12 MW corresponds to 4240 A of $I_d$. In order to analyze the dynamic response of the converter more profoundly, the 1.37 Mvar reactive reference signal is performed at $t = 1.1$ s equal to 1865 A of $I_q$, as shown in Fig. 6, including the reference signals, exact switching circuit, averaged model and simplified model responses.

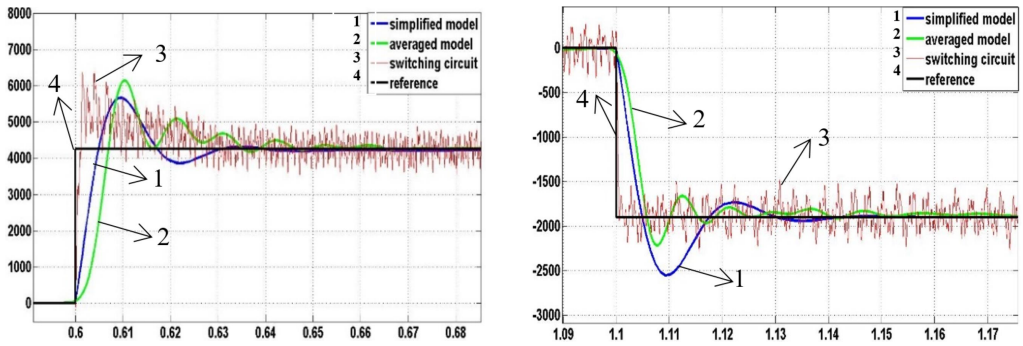


Fig. 6. $d$-$q$ components of ac-side current: $i_d(t)$ (a); $i_q(t)$ (b)

The behavior of ac-side states, the dynamic response of $i_d(t)$ and $i_q(t)$, are different for both the averaged model and exact switching circuit, as expected from (30). The various value of overshoots with respect to reference signals are justified by the presence of $L$. As a matter of fact, the inductance $L$ is reluctant to rapid set point changes. It causes more overshoot in the dynamic response of $i_d(t)$, which is the representative of active power, while the response of $i_q(t)$ encounters less overshoot, because of the fact that there is no need to provide energy from the dc source. Therefore, the inductance $L$ does not participate in reactive power provision. It follows the reference signal smoother. The differential equation of $i_q(t)$ from (30) is obviously proving this fact by noting the nonlinear part. $\delta$ is mostly small, which results in neglecting its nonlinear part responsible for the effect of dc-side states on $i_q(t)$.

### 6.2. Impact of mpedance network

As predicted before, the influence of the inductance $L$ on the behaviour of the system is allocated to $i_d(t)$. For proving it, the previous scenario for implementing active and reactive power signals is held for the ZSC system for different inductances, as shown in Fig. 7. The

overshoot of $i_{\mathrm{d}}(t)$ for smaller inductance is larger, because the larger one is the more reluctant to rapid changes in its current, At the same time, the response of $i_q(t)$ is completely independent of the inductance.

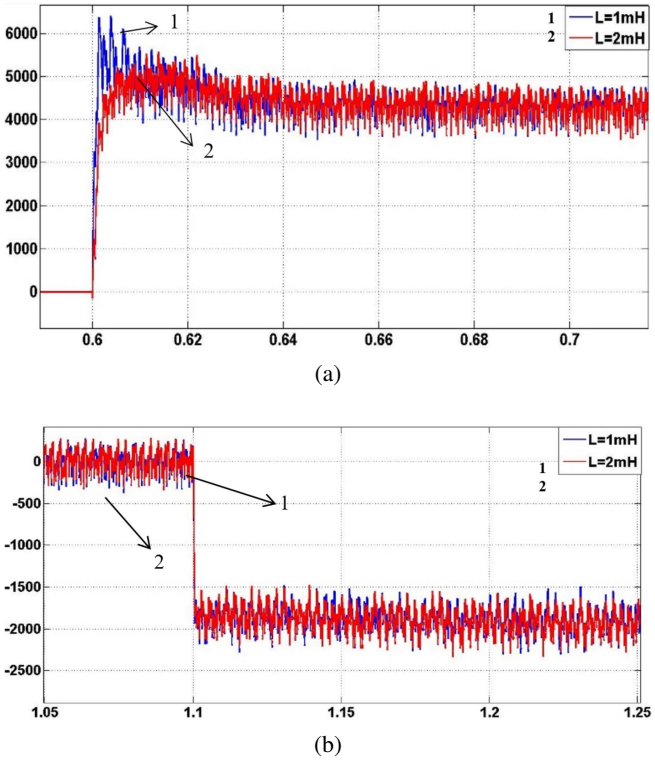


Fig. 7. Impact of dc-side inductance value on: $I_d$ (a); $I_q$ (b)

The effect of various capacitances and inductances on the behavior of capacitor voltage is shown in Fig. 8. At $t = 0.6$ s, the reference value of $I_d$ is changed, the response of capacitor voltage

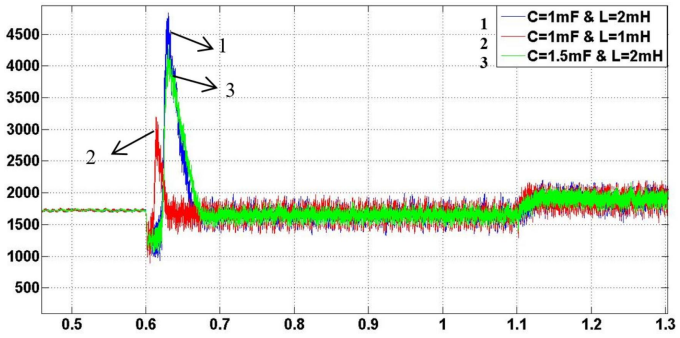


Fig. 8. Impact of capacitance and inductance on capacitor voltage dynamic response

is significantly more intensive compared with $t = 1.1$ s. It implies that at the first moments of changing the active power set point, the inductance $L$ is obstructing the path of energy. Therefore, the capacitor should provide the needed amount of energy, resulting in large dynamics and stresses that directly depend mainly on the inductance, and secondly on capacitance.

Table 1. Parameters of the study system in Fig. 1

| Parameter name | Symbol | Value | Unit |
|---|---|---|---|
| Rated active power | $P_s$ | 3.12 | MW |
| Rated reactive power | $Q_s$ | 1.3 | Mvar |
| AC grid nominal voltage | $V_s$ | 600 | V |
| AC equivalent inductance | $L_s$ | 100 | mH |
| AC equivalent resistance | $Rs$ | 1.63 | mΩ |
| Nominal frequency | $F$ | 60 | Hz |
| DC capacitance | $C$ | 1000 | μF |
| DC inductance | $L$ | 1 | mH |
| Nominal dc voltage | $V_{\mathrm{dc}}$ | 1250 | V |
| Current controller | $K_p$ | 0.022 | Ω |
| Current controller | $K_i$ | 5 | Ω/s |
| Carrier frequency | $F_s$ | 1 | kHz |

## 7. Conclusions

The simulations on the circuit of Fig. 1 have proved that the dynamic behavior of the ZSC connected to the ac grid system with any dc power can be persuasively simulated by the generalized dynamic model proposed in this paper. Moreover, the property and accuracy of the proposed controllers which are typical for VSC active and reactive current controllers are acquired through the simulation of the exact switching model. At first, basic average equations of the converter and its controllers are derived with regard to two individual operation modes, shoot-through and non-shoot-through states. By combining all the equations, a general nonlinearity and simplification are obtained, under some assumptions. In addition, in order to assess the impact of important parameters such as PI coefficients and impedance network components on the stability of the system, the small signal stability method is applied and the block diagram of the whole system is proposed. The main contribution of this paper is that the well-accurate general model for describing the dynamic response of the ZSC regardless of the type of dc power source and the direction of active power flow is derived. The model is perfectly suited for the study of AC/DC high-power equipment such as distributed generation and renewable energy systems. The effectiveness of the ZSC can be assessed on HVDC-light and FACTS equipment for future works.

**Acknowledgements**

The authors are very grateful for the cooperation and financial support of Neyriz Ghadir Steel Complex(NGHSCO), Shiraz University of Technology as well as Shiraz Electric Distribution Company.

**References**

[1] Peng F.Z., *Z-source inverter*, IEEE Trans. Ind Appl., vol. 39, no. 2, pp. 504–510 (2003), DOI: 10.1109/IAS.2002.1042647.

[2] Siwakoti Y.P., Peng F.Z., Blaabjerg F., Loh P.C., Town G.E., *Impedance-source networks for electric power conversion part I: a topological review*, IEEE Trans. Power Electron., vol. 30, no. 2, pp. 699–716 (2015), DOI: 10.1109/TPEL.2014.2313746.

[3] Siwakoti Y.P., Peng F.Z., Blaabjerg F., Loh P.C., Town G.E., Yang S., *Impedance-source networks for electric power conversion part II: review of control and modulation techniques*, IEEE Trans. Power Electron., vol. 30, no. 4, pp. 1887–1906 (2015), DOI: 10.1109/TPEL.2014.2329859.

[4] Peng F.Z., Yuan X., Fang X., Qian Z., *Z-source inverter for adjustable speed drives*, IEEE Trans. Power Electron., vol. 1, no. 2, pp. 33–35 (2003), DOI: 10.1109/LPEL.2003.820935.

[5] Peng F.Z., Joseph A., Wang J., Shen M., Chen L., Pan Z., Rivera E.O., Huang Y., *Z-source inverter for motor drives*, IEEE Trans. Power Electron., vol. 20, no. 4, pp. 857–863 (2005), DOI: 10.1109/TPEL.2005.850938.

[6] Shen M., Joseph A., Wang J., Peng F.Z., Adams D.J., *Comparison of traditional inverters and Z-source inverter for fuel cell vehicles*, IEEE Trans. Power Electron., vol. 22, no. 4, pp. 1453–1463 (2007), DOI: 10.1109/TPEL.2004.1393815.

[7] Guo F., Fu L., Lin C.H., Li C., Choi W., Wang J., *Development of an 85-kW bidirectional quasi-Z-source inverter with DC-link feed forward compensation for electric vehicle applications*, IEEE Trans. Power Electron., vol. 28, no. 12, pp. 5477–5488 (2013), DOI: 10.1109/TPEL.2012.2237523.

[8] Peng F.Z., Shen M., Holland K., *Application of Z-source inverter for traction drive of fuel cell-battery hybrid electric vehicles*, IEEE Trans. Power Electron., vol. 22, no. 3, pp. 1054–1061 (2007), DOI: 10.1109/TPEL.2007.897123.

[9] Dehghan S.M., Mohamadian M., Yazdani A., *Hybrid electric vehicle based on bidirectional z-source nine-switch inverter*, IEEE Trans. Vehicular Tech., vol. 59, no. 6, pp. 2641–2653 (2010), DOI: 10.1109/TVT.2010.2048048.

[10] Gajanayake C.J., Vilathgamuwa D.M., Loh P.C., Teodorescu R., Blaabjerg F., *Z-source-inverter-based flexible distributed generation system solution for grid power quality improvement*, IEEE Trans. Energy Convers., vol. 24, no. 3, pp. 695–704 (2009), DOI: 10.1109/TEC.2009.2025318.

[11] Jokar Kouhanjani M., Seifi A.R., Mehrtash M., *Dynamic Model and Small Signal Analysis of Z-Source Inverter*, IETE Journal of Research, vol. 66, no. 65:3, pp. 342–350 (2018), DOI: 10.1080/03772063.2018.1432421.

[12] Jokar Kouhanjani M., Seifi A.R., *Comparison of VSC and Z-source converter: power system application approach*, Advances in Electronic and Electric Engineering, vol. 15, no. 1, pp. 12–18 (2017), DOI: 10.15598/aeee.v15i1.1766.

[13] Ge B., Abu-Rub H., Peng F.Z., Li Q., de Almeida A.T., Ferreira F.J.T.E., Sun D., Liu Y., *An energy stored quasi-Z-source inverter for application to photovoltaic power system*, IEEE Trans. Ind. Electron., vol. 60, no. 10, pp. 4468–4481 (2013), DOI: 10.1109/TIE.2012.2217711.

[14] Dehghan S.M., Mohamadian M., Varjani A.Y., *A new variable-speed wind energy conversion system using permanent-magnet synchronous generator and z-source inverter*, IEEE Trans. Energy Convers., vol. 24, no. 3, pp. 714–724 (2009), DOI: 10.1109/TEC.2009.2016022.

[15] Jung J.W., Keyhani A., *Control of fuel cell based z-source converter*, IEEE. Trans. Energy Convers., vol. 22, no. 2, pp. 467–476 (2007), DOI: 10.1109/TEC.2006.874232.

[16] Liu J., Hue J., Xu L., *Dynamic modelling and analysis of z source converter-derivation of ac small signal model and design-oriented analysis*, IEEE Trans. Power Electron., vol. 22, no. 5, pp. 1786–1796 (2007), DOI: 10.1109/TPEL.2007.904219.

[17] Yu K., Luo F.L., Zhu M., *Study of an improved z-source inverter: small signal studies*, in Proc., 5th Annual IEEE Industrial Electronics and Application. Conf., pp. 2169–2174 (2010), DOI: 10.1109/ICIEA.2010.5515153.

[18] Gajanayake C.J., Vilathgamuwa D.M., Loh P.C., *Small- signal and signal-flow-graph modelling of switched z-source impedance network*, IEEE Lett. Power Electron., vol. 3, no. 3, pp. 111–116 (2005), DOI: 10.1109/LPEL.2005.859771.

[19] Loh P.C., Vilathgamuwa D.M., Gajanayake C.J., Lim Y.R., Teo C.W., *Transient modelling and analysis of pulse-with-modulated z-source inverter*, IEEE Trans. Power Electron., vol. 22, no. 2, pp. 498–507 (2007), DOI: 10.1109/TPEL.2006.889929.

[20] Galigekere V.P., Kazimierczuk M.K., *Analysis of PWM z-source DC-DC converter in CCM for steady state*, IEEE Trans. Circuits and Systems, vol. 59, no. 4, pp. 854–863 (2012), DOI: 10.1109/TCSI.2011.2169742.

[21] Galigekere V.P., Kazimierczuk M.K., *Small-signal modelling of open-loop PWM z-source converter by circuit-averaging technique*, IEEE Trans. Power Electron., vol. 28, no. 3, pp. 1286-1296, Mar. 2013, DOI: 10.1109/TPEL.2012.2207437.

[22] Peng F.Z., Shen M., Qian Z., *Maximum Boost Control of the Z-Source Inverter*, IEEE Trans. Power Electron, vol. 20, no. 4, pp. 833–838 (2005), DOI: 10.1109/TPEL.2005.850927.

[23] Shen M., Wang J., Joseph A., Peng F.Z., Tolbert L.M., Adams D.J., *Maximum constant boost control of the z-source inverter*, IEEE Indus. Appl. Conf., pp. 3–7 (2004), DOI: 10.1109/IAS.2004.1348400.

[24] Ding X., Qian Z., Xie Y., Peng F.Z., *A Novel ZVS Z-Source Rectifier*, IEEE Power Electron. Specialists Conf., pp. 1–5 (2006), DOI: 10.1109/APEC.2006.1620653.

[25] Yazdani A., Irevani R., *Voltage-sourced converters in power systems*, 1st ed., IEEE Press, John Wiley & Sons, pp. 204−244 (2010).

[26] Yazdani A., Irevani R., *An accurate model for the DC-side voltage control of the neutral point diode clamped converter*, IEEE Trans. Power Del., vol. 21, no. 1, pp. 185–193 (2006), DOI: 10.1109/TPWRD.2005.852342.

[27] Yazdani A., Iravani R., *A generalized state-space averaged model of the three-level NPC converter for systematic DC-voltage-balancer and current-controller design*, IEEE Trans. Power Del., vol. 20, no. 2, pp. 1105–1114 (2005), DOI: 10.1109/TPWRD.2004.834307.

[28] Liang H., Li G., Li P., Yin M., *Analysis and design of H1 controller in VSC HVDC systems*, in: IEEE/PES Transmission and Distribution Conference and Exhibition: Asia and Pacific, p. 6 (2005), DOI: 10.1109/TDC.2005.1547069.

[29] Zhang L., Nee H.-P., *Multivariable feedback design of VSC-HVDC connected weak AC systems*, in: Power Tech., pp. 1–8 (2009), DOI: 10.1109/PTC.2009.5282110.

[30] Li G., Ma G., Zhao C., Li G., *Research of nonlinear control strategy for VSC-HVDC system based on Lyapunov stability theory*, in Proc. 3rd International Conference on Electric Utility Deregulation and Restructuring and Power Technologies, pp. 2187–2191 (2008), DOI: 10.1109/DRPT.2008.4523773.

[31] Mao C., Hu Z., Lu J., Chang D., Fan S., *Application of an optimal coordinated control strategy to VSC HVDC*, in Proc. IEEE PES Power Systems Conference and Exposition, pp. 2141–2145 (2006), DOI: 10.1109/PSCE.2006.296275.

[32] Tsang K.M., Chan W.L., *Decoupling controller design for z-source inverter*, IET Power Elec., vol. 8, no. 4, pp. 536–545 (2015), DOI: 10.1049/iet-pel.2014.0207.